SINGLE NEUTRON COUNTING USING CCD AND CMOS CAMERAS

P. Mutti*, E. Ruiz-Martinez, M. Platz, P. Van Esch
Institut Laue-Langevin, Grenoble, France
M. Crisanti, Universitá degli studi di Perugia, Perugia, Italy

Abstract

The present paper explores the technical possibility to use classical imaging detectors such as Charge-Coupled Devices (CCD) and Complementary Metal-Oxide Semiconductor (CMOS) cameras as counting detectors at lower counting rates and transits smoothly to continuous imaging at higher rates. The gamma-rejection capabilities as well as the counting efficiency have been investigated with both an AmBe neutron source and in-beam experiments.

INTRODUCTION

Neutrons have mass but no electrical charge. Because of this they cannot directly produce ionisation in a detector, and therefore cannot be directly detected. This means that neutron detectors must rely upon a conversion process where an incident neutron interacts with a nucleus to produce a secondary charged particle. Classical neutron detectors are based upon particle detection technologies like gas filled proportional counters or scintillation detections. These detectors have a high dynamic range, and are very performing at low counting rates and fast timing (time-of-flight) applications. At high counting rates however, continuous imaging detectors such as CCD or CMOS camera's optically linked to scintillators, can have very good performances concerning linearity and spatial resolution but the dynamic range of these systems is limited by electronic noise and gamma background.

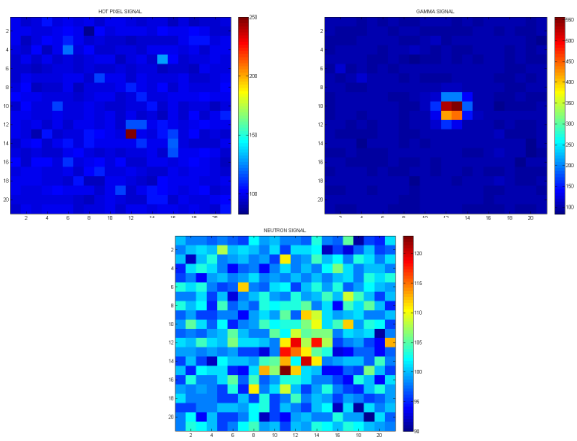

Figure 1: Different light patterns in a CMOS camera.

The capability of single neutron counting relies on the possibility to distinguish the neutron signature on the camera from those belonging to gammas or electronic noise (hot pixel). Neutron detection involves reactions releasing energies of the order of the MeV, while X-ray detection releases energies of the order of the photon energy ($\sim$10 keV). This 100-fold higher energy released in the interaction, transforms into a much different light yield allowing the individual neutron light signal to be significantly above the noise level and therefore opening the possibility for gamma-discrimination and individual counting. Figure 1 shows the different light patters obtained using our CMOS camera. The *hot pixel* is shown in the left-upper plot, the gamma detection in the right-upper and the neutron signature in the lower one.

NEUTRON RECOGNITION

^{3}He based proportional gas neutron detectors have an impressive gamma rejection ratio in the range from 10^{-6} to 10^{-8} [1]. This impressive noise rejection ratio comes from a non-linear operation, called discrimination. The noisy analogue signal is put to 0 in the end result, as long as it doesnt cross a threshold. In such a way, all the integrated noise (whether electronic noise, inherent detector noise, or gamma radiation) is eliminated entirely. If one assumes a Gaussian noise with a standard deviation σ and a threshold set at 6σ, the probability per independent sample (about every μs) to cross that positive threshold equals about 10^{-9} which gives a background rate of 10^{-3} counts/s. At a count rate of 10 neutrons per second, an integrating detector summing all the samples over a period of 1 second would have a total signal of about 60σ (assuming the individual signal level equal to 6σ) and a noise level equal to 1000σ: in other words, the signal would be entirely swamped by the noise. When used in classical integrating imaging mode, a CMOS like camera suffers a similar degradation of the final signal-to-noise ratio and, therefore, it can only really be used when the neutron fluxes are very intense, such as in neutrography, or in Laue diffraction. Normally, the camera pixel size is smaller than the size of the typical light spot from a neutron scintillator event on the camera and, therefore, one can assume that the scintillating light has a 2-dimensional Gaussian distribution as shown in Fig. 2.

We will consider a re-pixelisation where we combine the camera pixels into what we call *spot pixels*: pixels that are about the size of the FWHM of this Gaussian distribution. We take images with such short exposure times that the amount of noisy photo-electrons in a spot pixel is well below the expected number of photo- electrons corresponding to a neutron scintillation event, and we put a threshold that distinguishes them. The first problem related to this

* mutti@ill.eu

ISBN 978-3-95450-148-9

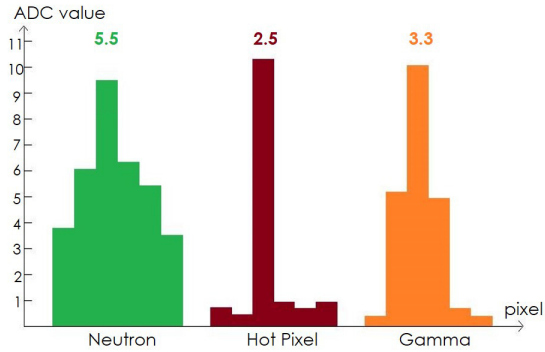

Figure 2: Pixel profiles for neutrons, hot pixels and gammas.

approach is that if more than one neutron impacts a certain spot pixel, we will nevertheless only count a single neutron. This means, essentially, that our system has a local non-paralysable dead time which is of the order of the exposure time. The second problem is that the neutron impacts will not coincide with the centres of the spot pixels. To solve the second problem, we assume that the probability of the location of impact of a single neutron on a spot pixel is uniformly distributed over the area of that pixel. We then pick a threshold so that statistically, we miss just as many neutron impacts as we double count others. This hypothesis is valid if the resolution given by the spot pixel is smaller than the features in the image. This is the case if the detector is not the resolution-limiting part of the instrument.

SIMULATION

A Monte Carlo simulation is performed in which a constant amount of light is distributed according to a Gaussian profile with a FWHM equal to the width of individual spot pixels, and with uniformly distributed centre position. Varying the threshold value as a percentage of the intensity of a neutron flash, the ratio of the number of neutrons counted over the number of neutron flashes simulated, is shown in Fig. 3.

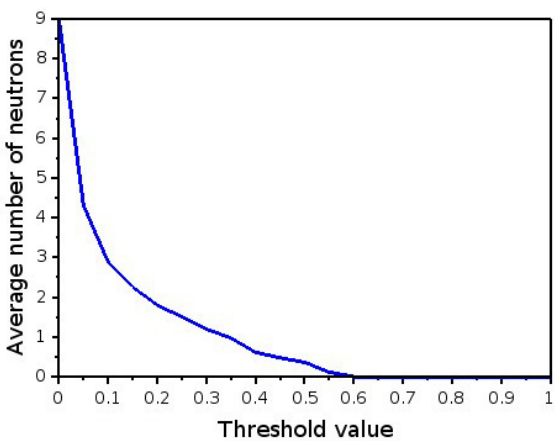

Figure 3: Average number of neutron counts for a single neutron impact of light intensity as a function of the threshold value.

As expected, for a low value of the threshold, neutrons are over-counted, namely a single neutron will trigger a count in several neighbouring pixels. For a high value of the threshold, not all neutrons are counted. But for a threshold equals to 34% of the full intensity, on average, one neutron is counted per neutron impact. More precisely, about 80% of the neutrons are correctly counted as a single neutron, while about 10% is not counted, and another 10% is counted twice. To tackle the first problem, we propose to use a function $f(e)$ that indicates, how many neutrons we should count as a function of the amount of photo-electrons in the spot pixel. Its asymptotic behaviour should be:

$$\lim_{e\to\infty} f(e) \to \frac{e}{e_n} \tag{1}$$

where e_n is the average total number of photo-electrons per single neutron impact. Near the threshold value te_n the function should be near 1. We have considered 2 different functions. The first equals the integrating value if the charge in a pixel is larger than a full neutron charge, otherwise, the threshold fraction t of e_n is applied to decide if one should count a neutron or not:

$$\begin{aligned} f(e) &= [\frac{e}{e_n}] \quad ; \quad e > e_n \\ f(e) &= 1 \quad ; \quad e_n > e > te_n \\ f(e) &= 0 \quad ; \quad te_n > e \end{aligned} \tag{2}$$

This function implements most closely the separation between single neutron counting and continuous charge integration. The second function is smoother, and applies the following prescription:

$$f(e) = \frac{e}{e_n} + (1 - t) \tag{3}$$

Applying both functions to our simulation resulted in a slight over-counting when the neutron density is between 0.1 and 10 neutrons per spot pixel. This error can be as big as 20% but can be corrected a posteriori once the average neutron density is known.

EXPERIMENTAL SETUP

Individual neutron counting with CCD-like cameras has already been reported [2], but image intensifiers were necessary to bring the light flash to a detectable level. What is relatively new, are fast CMOS cameras that allow up to 100 fps, of which the noise properties are sufficiently good, and the quantum efficiency sufficiently high to allow for the threshold application without prior light amplification. All the measurements presented in this paper were carried out using an ORCA-Flash4.0 V2 CMOS camera from Hamamatsu [3]. This camera is equipped with a 4 Mpixel CMOS image sensor adopting an on-chip column amplifier and ADC converter to achieve higher speed, performing simultaneous parallel signal readout. This allows low-noise and high-speed readout. The camera achieves

ISBN 978-3-95450-148-9

both the low noise of 1.0 electron (median) and 1.6 electrons (rms), and the high frame rate of 100 frames/s (at 2048 × 2048 pixels). The camera is coupled with a 50 mm f/0.95 MVL50HS objective by Thorlabs. For the neutron detection we used a ZnS(Ag) scintillator screen of a thickness of 200 μm on a 0.5 mm thick aluminium substrate from Applied Scintillation Technologies. In the scintillator, the ZnS powder is mixed with LiF in the proportion 2:1. The ^{6}Li capture a neutron with the reaction:

$$^6Li + n \rightarrow \alpha + ^3H + 4.8MeV \quad (4)$$

where the 4.8 MeV produced are shared between the α (2.05 MeV) and the tritium (2.74 MeV). The ZnS is activated by Ag that creates empty level nearby the conduction and the valence band of the ZnS. α particles or a tritium produce ionisation creating electron-hole pairs. When these couples make a transition from an excited state to the ground state, they emit photons in the visible range. The camera was first used with a 3.7 GBq Am-Be source which provides neutrons with a smooth energy distribution centred around 4 MeV. Those neutrons are subsequently moderated by a thick layer of polyethylene surrounding the source to move the neutron spectrum towards thermal energy. The source emission is nevertheless dominated by a strong gamma flux at 4.4 MeV resulting from the de-excitation of ^{12}C. Final tests have been performed on the T13C [4] beam line. A neutron beam of about 10^9 n·cm^2/s was diffracted by a Ge (111) perfect crystal monochromator. The intensity of the monochromatic beam at 3.26 Åhitting the scintillator was in the order of 10^5 n·cm^2/s.The total beam size was 50×30 mm^2. We have measured the neutron detection efficiency of the scintillator by mean of a reference 100% efficiency ^{3}He detector. The ratio of neutron counts with the aluminium support alone and Al plus ZnS resulted in a 12% efficiency at 3.26Å.

TEST WITH Am-Be SOURCE

For the first test we have exposed the ZnS(Ag) scintillator to an AmBe neutron source (see previous chapter for details). The CMOS camera was looking only partially at the scintillator in order to have clearly a region were no neutron signals should be present. The goal of those first measurements was to find out whether individual neutron detection is possible, how much photo-electrons are collected and whether a threshold-based algorithm can discriminate genuine neutron signals from other noise events. series of images were taken, varying the distance between camera and scintillator from 5 to 10 and 20 cm.

The first processing removes hot pixels which are due to the CMOS technology imperfections and also to the direct gamma impacts from the AmBe source on the camera sensor itself. The second processing recognises individual neutron flashes in order to study them. With the AmBe source, the neutron flux is very low and no measurements in integration mode were possible. Figure 4 report the obtained results. The left side represent the raw image before any

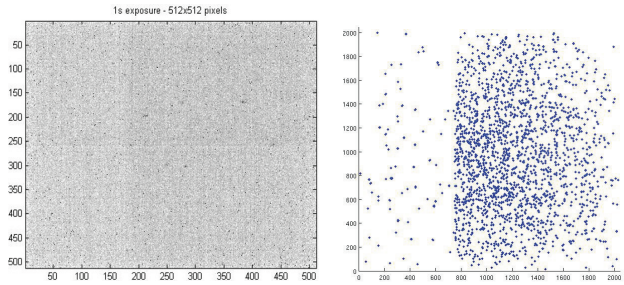

Figure 4: Neutron recognition after partial illumination of the scintillator with the AmBe source.

treatment, while the right side shows the recognised neutrons cumulated over 400 images. One can notice how the majority of neutrons sit on the scintillator side and only a few impacts are located on the side without scintillator. The border of the scintillator is, as well, clearly seen. A second validation comes from the fact that the number of neutrons detected increases proportionally to exposure time. Finally, removing the AmBe source lowers drastically the number of detected neutrons. Given the low intensity of the neutron source, we used exposure times which are longer than we would ideally prefer, in order to have sufficient neutron impacts in a reasonable amount of images.

IN-BEAM TEST

For this series of measurements the CMOS camera was placed inside a black box at 90^o with respect to the incoming neutron beam to avoid a direct view of the beam. The 50 mm objective is focused on the scintillator via a 45^o mirror obtained by coating a glass plate with titanium.

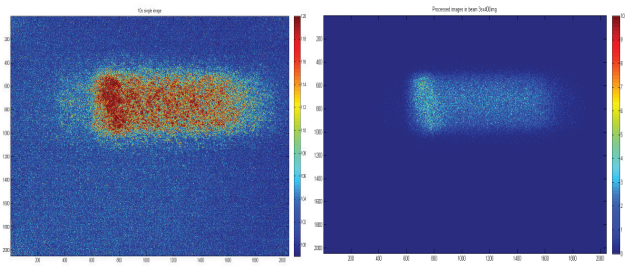

Figure 5: T13C beam profile. Left part is a single image of 10 s exposure, right part is the algorithm reconstruction.

Left part of Fig. 5 shows the beam profile obtained with the CMOS camera in normal integration mode and with an exposure of 10 s. The right part of Fig. 5 represent the result of our algorithm after the processing of 400 images with an exposure time of 50 ms each. A clear asymmetry in the neutron beam is present on both the direct and the reconstructed image. This effect was probably due to a non perfect alignment of the monochromator crystal with respect to the detector. One can notice as well how the reconstruction places all neutrons within the beam area. Also in this case we varied the exposure time to verify the

ISBN 978-3-95450-148-9

ity of the neutron identification and the results will be discussed in the next chapter.

RESULTS

it is reasonable to expect a linear increase of detected neutrons when increasing the exposure time per image. If this is clearly the case for the measurements performed with the AmBe source, this linearity is not maintained for the beam measurements as one can see in Fig. 6 (blue circles), where the counted neutrons are clearly overestimated.

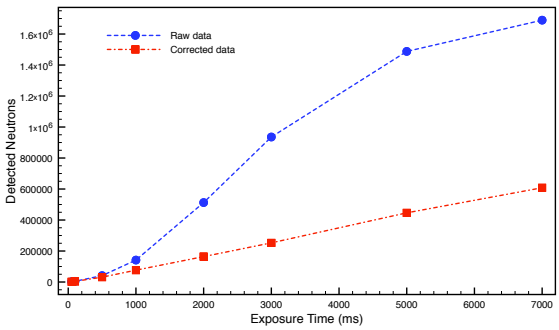

Figure 6: Counted neutrons as a function of the exposure time. Blue circles represent data from original images while red squares are obtained after removal of double counting.

From every single image we calculated the nearest neighbour distance in spot pixel between detected neutrons. This distribution is dominated by a value of 1 pixel which implies the fact that we are probably double counting neutrons. To prove this theory we have simulated a neutron distribution having the same density than the real image. Calculating again the nearest neighbour distance, the possibility of 1 pixel distance is not disappeared but now the peak value is at 4 pixels (see Fig. 7).

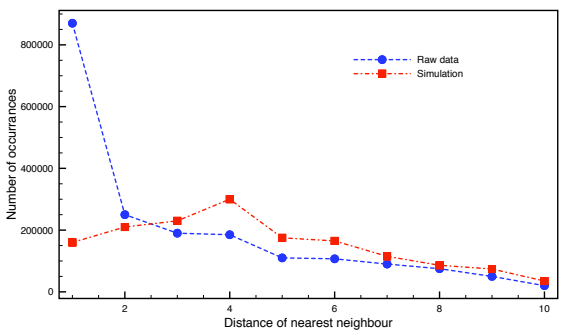

Figure 7: Shortest distance between 2 recognised neutrons. Blue circles represent data from original images while red squares are obtained from the simulated distribution.

After statistical removal of the artificial double counting we obtained the red squares curve reported in Fig. 6 where the linearity is reestablished. A possible explanation is related to the high sensitivity of the algorithm to the threshold parameter. At high neutron density the probability of multiple impacts on nearby pixels increases. The signals are than spread over a number of contiguous spot pixels which are interpreted as double counts. It becomes evident that to be able to exploit the single neutron counting algorithm one has either to consider only low neutron density or increase the camera frame rate to limit, in such a way, the total number of neutrons per frame.

CONCLUSION

Starting from the theoretical concept that a threshold-based neutron counting system can in principle be obtained using a CMOS camera looking at a scintillator, we verified experimentally that single neutron impacts could indeed be identified using an AmBe source as well as in a beam experiment. The recent advances in camera technology now permit us with a commercial camera at relatively low cost, and without the need of light amplification, to detect individual neutrons. This is sufficient justification to invest deeper into the question of a camera-based neutron counting detection system, as in principle, it can combine the good background rejection and the capability to sustain very low count rates, which is typical of neutron counting detectors, with the classical advantages of integrating detectors, such as absence of dead time and hence the capacity to sustain very high local count rates, and high spatial resolution. The beam measurements have shown the problems related to the double counting when the neutron flux increases pointing out the need for a high image rate to reduce the number of neutrons per single frame.

This work would have not been possible without the technical support of Neutron Optics department at the Institut Laue-Langevin. In particular the authors would like to thank Dr. Pierre Courtois for the help in setting up and running the measurements on the T13C beam line.

REFERENCES

[1] Institut Laue-Langevin (2012), France, "T13C high resolution diffractometer", http://www.ill.eu

[2] Hamamatzu (2015), Japan, "ORCA-Flash4.0 V2 Digital CMOS camera", http://www.hamamaztu.com

[3] M. Dietze et al., Nucl. Instr. Meth. A, 377 (1996) 320-324

[4] Kouzes et al., Nucl. Instr. Meth. A, 654 (2011) 412-416

ISBN 978-3-95450-148-9